Journal of Pathology
J Pathol 2015; **237:** 520–531
Published online 28 September 2015 in Wiley Online Library (wileyonlinelibrary.com) DOI: 10.1002/path.4597

ORIGINAL PAPER

Loss of RUNX3 expression promotes cancer-associated bone destruction by regulating CCL5, CCL19 and CXCL11 in non-small cell lung cancer

Hyun-Jeong Kim,[1,2] Junhee Park,[2] Sun Kyoung Lee,[1,2] Ki Rim Kim,[3] Kwang-Kyun Park[1,2]* and Won-Yoon Chung[1,2]*

[1] *Department of Oral Biology, Oral Cancer Research Institute, BK21 PLUS Project, Yonsei University College of Dentistry, 50-1 Yonsei-ro, Seodaemun-gu, Seoul, Korea*
[2] *Department of Applied Life Science, The Graduate School, Yonsei University, 50 Yonsei-ro, Seodaemun-gu, Seoul, Korea*
[3] *Department of Dental Hygiene, Kyungpook National University, Sangju, Korea*

**Correspondence to: W-Y Chung, Department of Oral Biology, Yonsei University College of Dentistry, 50–1 Yonsei-ro, Seodaemun-gu, Seoul 120–752, Korea. E-mail: wychung@yuhs.ac*
Or K-K Park, Department of Oral Biology, Yonsei University College of Dentistry, 50–1 Yonsei-ro, Seodaemun-gu, Seoul 120–752, Korea. E-mail: biochelab@yuhs.ac

Abstract

Non-small cell lung cancer (NSCLC) frequently metastasizes to bone, which is associated with significant morbidity and a dismal prognosis. RUNX3 functions as a tumour suppressor in lung cancer and loss of expression occurs more frequently in invasive lung adenocarcinoma than in pre-invasive lesions. Here, we show that RUNX3 and RUNX3-regulated chemokines are linked to NSCLC-mediated bone resorption. Notably, the receptor activator of nuclear factor-κB ligand (RANKL)/osteoprotegerin (OPG) ratio, an index of osteoclastogenic stimulation, was significantly increased in human osteoblastic cells treated with conditioned media derived from RUNX3-knockdown NSCLC cells. We aimed to identify RUNX3-regulated factors that modify the osteoblastic RANKL/OPG ratio and found that RUNX3 knockdown led to CCL5 up-regulation and down-regulation of CCL19 and CXCL11 in NSCLC cells. Tumour size was noticeably increased and more severe osteolytic lesions were induced in the calvaria and tibiae of mice that received RUNX3-knockdown cells. In response to RUNX3 knockdown, serum and tissue levels of CCL5 increased, whereas CCL19 and CXCL11 decreased. Furthermore, CCL5 increased the proliferation, migration, and invasion of lung cancer cells in a dose-dependent manner; however, CCL19 and CXCL11 did not show any significant effects. The RANKL/OPG ratio in osteoblastic cells was increased by CCL5 but reduced by CCL19 and CXCL11. CCL5 promoted osteoclast differentiation, but CCL19 and CXCL11 reduced osteoclastogenesis in RANKL-treated bone marrow macrophages. These findings suggest that RUNX3 and related chemokines are useful markers for the prediction and/or treatment of NSCLC-induced bone destruction.

Keywords: RUNX3; RUNX3-regulated chemokines; non-small cell lung cancer; cancer-mediated bone resorption; RANKL; osteoprotegerin

Received 22 December 2014; Revised 10 July 2015; Accepted 22 July 2015

No conflicts of interest were declared.

Introduction

Non-small cell lung cancer (NSCLC) accounts for approximately 80% of lung cancers and has an overall 5-year survival rate of only 15%. Bone metastases occur in 30–40% of NSCLC patients and develop skeletal-related events, resulting in negative effects on quality of life and survival [1]. Lung cancer metastasis to bone is the primary cause of osteolytic lesions in the spine, ribs, pelvis, and proximal long bones. These lesions arise due to functional interactions between cancer cells and bone cells [2,3]. Localized cancer cells within the bone produce several osteoclastogenic factors directly or via cancer–stroma interactions. These factors converge on pre-osteoblasts/stromal cells to increase the expression of receptor activator of nuclear factor-κB ligand (RANKL) and/or to decrease the expression of its decoy receptor osteoprotegerin (OPG). RANKL binds to its receptor RANK on osteoclast precursors and induces osteoclastogenesis, causing increased bone resorption [3–5]. The growth factors released from the degraded bone matrix further stimulate the growth of cancer cells and promote the secretion of their osteolytic factors, leading to a 'vicious cycle' of bone destruction and metastatic outgrowth [5,6]. Unfortunately, little is known about the factors involved in lung cancer-mediated bone destruction and the mechanisms by which osteolytic lesions are formed.

Human runt-related transcription factor (RUNX) proteins have pivotal functions in normal development and the development of neoplasia [7]. In cancer-related bone diseases, RUNX2 has taken centre stage as a pro-metastatic factor and potential target for controlling metastatic breast and prostate cancer cells in the bone microenvironment because it is critical for the regulation of genes that support bone formation and because it is abnormally expressed in tumours with bone tropism [8]. In contrast, RUNX3 acts a tumour suppressor in most cancers [9]. Aberrant methylation of the *RUNX3* gene promoter occurs during carcinogenesis and is more frequent in invasive than in pre-invasive lung adenocarcinoma lesions [10,11]. *RUNX3* methylation correlates with clinical stage, lymph node metastasis, and degree of differentiation in NSCLC [12]. In addition, murine Runx3 cooperates with Runx2 to induce chondrocyte maturation [13], and increased *RUNX3* promoter methylation is associated with aggressive chondrosarcoma and decreased survival time [14].

Chemokines are small secreted proteins that attract and activate cells to specific locations in the body under both physiological and pathological conditions [15]. These proteins have a direct influence on tumour growth, invasion, and specific homing to metastatic sites [16], and they also mediate the crosstalk between tumour cells and bone microenvironment [17]. In lung cancer, tumour-derived IL-8 induces osteoclast differentiation via RANKL-dependent and RANKL-independent pathways, thereby stimulating osteolysis [18]. In contrast, CCL22 production by differentiating osteoclasts promotes the bone metastasis of lung cancer cells expressing its receptor CCR4 [19].

The aim of this study was to determine whether RUNX3 and RUNX3-regulated chemokines could serve as predictive markers and/or therapeutic targets of lung cancer-mediated bone diseases. We investigated the role of RUNX3 in NSCLC-mediated bone destruction and examined the effects of the RUNX3-regulated chemokines CCL5, CCL19, and CXCL11 on cancer cells, osteoblasts, and osteoclasts.

Materials and methods

Supplementary materials and methods include more details of reagents, antibodies, animals, cell culture, western blot analysis, RUNX3 knockdown, qRT-PCR, RT-PCR, PCR array of human chemokines and their receptors, and public database analysis.

Preparation of conditioned medium (CM)

shNC or shRUNX3 A549 and H838 cells were seeded at 2×10^6 cells per 100-mm dish and incubated overnight. The culture media were replaced with serum-free DMEM/F12 and the cells were cultured for 24 h. Culture media were collected and centrifuged at 500 *g* for 5 min. The supernatant (CM) was used for subsequent experiments.

Quantitative real-time RT-PCR (qRT-PCR), ELISA, and western blot

hFOB1.19 cells (5×10^6 cells per dish) were treated with CM for 6 h or incubated in serum-free media with the indicated concentrations of human CCL5, CCL19, or CXCL11 for 6 h. *RANKL* and *OPG* mRNA expression was examined by qRT-PCR as described in the Supplementary materials and methods. CCL5, CCL19, and CXCL11 levels in CM were measured with Quantikine human CCL5/RANTES and CXCL11/I-TAC immunoassay kits (R&D Systems, Minneapolis, MN, USA) and the CCL19 ELISA kit (Abnova, Taipei City, Taiwan) following the manufacturers' protocols. The total protein in the CM was determined using BCA protein assay reagents (Pierce, Rockford, IL, USA). For western blotting, hFOB1.19 cells were incubated for 6 h in serum-free medium containing 75% CM plus neutralizing antibodies against human CCL5, CCL19, or CXCL11. Cells were also treated with human CCL5, CCL19, or CXCL11 at the indicated concentrations. RANKL and OPG protein expression was determined with their specific primary antibodies as described in the Supplementary materials and methods.

A murine calvarial model of cancer-associated bone invasion and osteolysis

All animal experiments were approved by the Institutional Animal Care and Use Committee of the Department of Laboratory Animal Resources, Yonsei Biomedical Research Institute, Yonsei University College of Medicine (Approval No 2012–0044, 2012–0045). Six-week-old female BALB/c nude mice were randomly divided into three groups, with nine mice per group. shNC or shRUNX3 A549 cells (1×10^7 cells per 100 µl of PBS) were injected subcutaneously over the calvaria of the mice using a 1-ml syringe with a sterile 26-gauge needle. Control mice were injected with PBS alone. The volumes of tumours over the calvaria were measured twice per week using a digital electric caliper for 46 days and calculated according to the formula $(a \times b^2)/2$, where a is the longest diameter and b is the shortest diameter of the tumour. On day 46, blood, calvaria, and tumours were collected.

A murine intratibial model of cancer-associated bone resorption

Five-week-old female BALB/c nude mice were randomly divided into three groups, with seven mice per group. shNC or shRUNX3 A549 cells (1×10^6 cells per 50 µl of HBSS) were injected into the bone marrow of the right tibia through the femorotibial cartilage using a Hamilton syringe with a sterile 27-gauge needle. Control mice were injected with HBSS alone. On day 49, the mice were anaesthetized for µCT analysis of the tibiae. Blood and tibiae were collected.

μCT imaging and bone structure analysis

Bone morphometric parameters of the calvaria or tibiae were determined using a μCT analyser (SkyScan 1076; SkyScan, Aartselaar, Belgium) with NRecon software (SkyScan). Two-dimensional (2D) images were used to generate 3D reconstructions with the software supplied with the instrument [20,21].

Histological and immunohistochemical examination

Sections of calvaria and tibiae were prepared and stained with haematoxylin and eosin (H&E) as described previously [20,22]. To detect osteoclasts, sections were stained for TRAP using the Acid Phosphatase Leukocyte Kit (Sigma-Aldrich, St Louis, MO, USA). Multinucleated TRAP-positive cells along the tumour–bone interface were observed via microscopy (original magnification × 100). For immunohistochemical staining, the sections were deparaffinized, rehydrated, and treated with 3% hydrogen peroxide for 15 min at room temperature followed by treatment with goat serum for 30 min. The sections were incubated overnight at 4 °C with primary antibodies (diluted 1:50 or 1:300) against RUNX3, CCL5, CCL19, and CXCL11. The sections were treated with HRP-conjugated secondary anti-rabbit IgG antibodies (diluted 1:100) for 30 min. HRP was developed using the DAB system (Lab Vision Corporation, Fremont, CA, USA). The sections were counterstained with haematoxylin, dehydrated, mounted, and examined via microscopy.

Determination of serum biochemical parameters

Blood samples were maintained at room temperature for 1 h and then centrifuged at 900 *g* for 20 min to obtain serum. The serum levels of calcium, alkaline phosphatase (ALP), and osteoclast-derived TRAP5b were estimated using the QuantiChrome calcium assay kit, the ALP assay kit (BioAssay Systems, Hayward, CA, USA), and a mouse TRAP assay kit (Immunodiagnostic Systems, Scottsdale, AZ, USA) according to the manufacturers' instructions. The CCL5, CCL19, and CXCL11 levels in the serum were measured using their respective kits.

Cell viability, BrdU incorporation, and migration/invasion

The viability of shNC or shRUNX3 A549 cells was determined using the trypan blue exclusion assay, and that of bone marrow macrophages (BMMs) was measured with the MTT assay. DNA synthesis was measured in shNC or shRUNX3 A549 cells using a BrdU cell proliferation ELISA kit (Roche Diagnostics, Penzberg, Germany). The migratory and invasive abilities of shNC or shRUNX3 A549 cells were evaluated using a scratch migration assay and transwell invasion assay, respectively [21].

Osteoclast differentiation assay

BMMs (5×10^4 cells per well) were cultured in α-MEM containing 10% FBS, 30 ng/ml M-CSF, and 100 ng/ml RANKL in the absence or presence of CCL5, CCL19, or CXCL11 at the indicated concentrations for 5 days. The number of osteoclasts was determined by counting the number of multinucleated (≥3 nuclei) TRAP-positive cells [20,22].

Statistical analysis

The data are expressed as means ± standard error (SE). Statistical analyses were performed using one-way analysis of variance (ANOVA) and Student's *t*-test to evaluate differences between groups. $p < 0.05$ was considered statistically significant.

Results

RUNX3 knockdown in NSCLC cells increased the osteoblastic RANKL/OPG ratio by modulating the production of CCL5, CCL19, and CXCL11

To determine the role of RUNX3 in lung cancer-mediated bone destruction, we detected RUNX3 expression in two of four NSCLC cell lines (Supplementary Figure 1A) and established stable RUNX3-knockdown (shRUNX3) A549 and H838 cells via lentiviral vector-mediated transduction with RUNX3 shRNA (Supplementary Figure 1B). Treatment with CM from shNC (control) A549 cells increased the RANKL/OPG ratio in hFOB1.19 osteoblastic cells, an index of osteoclastogenesis stimulation, by inducing *RANKL* mRNA and reducing *OPG* mRNA. Moreover, *RANKL* mRNA and the RANKL/OPG ratio were increased at a substantially higher level in response to treatment with CM from shRUNX3 A549 cells (Figure 1A). RUNX3 knockdown in H838 cells also resulted in substantial increases in osteoblastic *RANKL* mRNA expression and the RANKL/OPG ratio (Figure 1B). In contrast, RUNX3 knockdown slightly increased the viability (Supplementary Figure 1C), migration (Supplementary Figure 1D), and invasion (Supplementary Figure 1E) of A549 lung cancer cells, as well as the amount of newly synthesized DNA in proliferating cells (Supplementary Figure 1C). These results suggest that RUNX3 knockdown in NSCLC cells may influence the production of factors that alter osteoblastic RANKL expression rather than their metastatic ability.

To identify RUNX3-regulated factors in NSCLC cells that control osteoblastic RANKL expression, we examined the mRNA levels of chemokines and their receptors in response to RUNX3 knockdown in A549 cells. RUNX3 knockdown resulted in up-regulation of *CCL5* and *TCP10* and down-regulation of *CXCL11*, *CCL19*, and *HCAR1* (Supplementary Table 1). ELISA analyses revealed that the level of secreted CCL5 increased by 1.8-fold (from 17.4 to 30.6 pg) but that

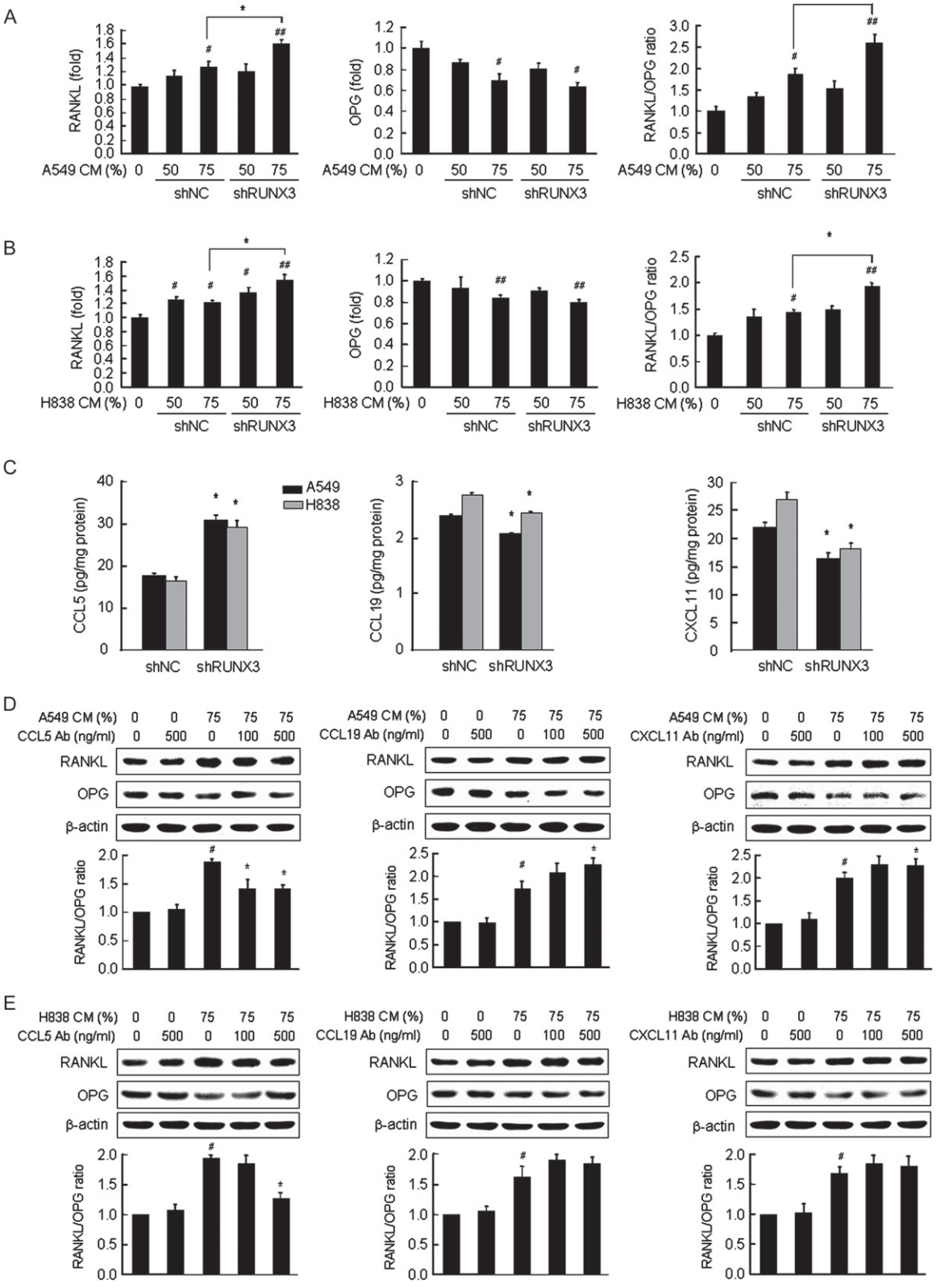

Figure 1. RUNX3 knockdown in NSCLC cells substantially increased the osteoblastic RANKL/OPG ratio by modulating NSCLC-derived chemokines. (A, B) The mRNA levels of RANKL and OPG were determined via qRT-PCR in hFOB1.19 cells treated with 50% and 75% CM from shNC or shRUNX3 A549 (A) and H838 cells (B) for 6 h. Mean ± SE; $^{\#}p < 0.05$, $^{\#\#}p < 0.01$ versus osteoblastic cells without CM; $^{*}p < 0.05$ versus osteoblastic cells treated with shNC cell-derived CM. (C) CCL5, CCL19, and CXCL11 in culture media of shNC or shRUNX3 A549 and H838 cells. Mean ± SE; $^{*}p < 0.05$ versus shNC cells. (D, E) hFOB1.19 osteoblastic cells were treated with 75% CM of A549 cells (D) or H838 cells (E) and the indicated concentrations of neutralizing antibodies against CCL5, CCL19 or CXCL11 for 6 h. RANKL and OPG protein were investigated via western blot analysis. The images are representative of three independent experiments. The graphs illustrate the ratio of the densitometric intensity of RANKL to that of OPG after normalization to β-actin. Mean ± SE; $^{\#}p < 0.01$ versus osteoblastic cells without CM and specific antibodies against chemokines; $^{*}p < 0.05$ versus CM-treated osteoblastic cells.

CCL19 and CXCL11 secretion decreased by 0.8-fold (from 2.4 to 2.1 pg) and 0.7-fold (from 22.7 to 16.1 pg), respectively, in culture medium from shRUNX3 A549 cells. Similar to A549 cells, RUNX3 knockdown in H838 cells also caused an increase in the level of CCL5 in the culture medium by 1.8-fold (from 16.3 to 29.3 pg) but decreased CCL19 and CXCL11 levels by 0.9-fold (from 2.8 to 2.4 pg) and 0.7-fold (from 26.9 to 18.0 pg), respectively (Figure 1C). In addition, RT-PCR data (Supplementary Figure 2A) and western blot analysis (Supplementary Figure 2B) indicated that RUNX3 knockdown increased *CCL5* mRNA and protein expression but decreased the mRNA and protein expression of CCL19 and CXCL11. Consistent with the array data, RUNX3 knockdown did not affect the mRNA levels of *CCR1*, *CCR3*, *CCR4*, *CCR5* (CCL5 receptors), *CCR7* (a CCL19 receptor), *CXCR3*, or *CXCR7* (CXCL11 receptors) (Supplementary Figure 3A) and did not change the protein levels of CCR5, CCR7, or CXCR3, which are recognized to be major receptors for CCL5, CCL19, and CXCL11, respectively, in A549 and H838 cells (Supplementary Figure 3B).

To verify whether CCL5, CCL19, and CXCL11 are NSCLC-derived factors that modulate osteoblastic RANKL and OPG expression, hFOB1.19 cells were treated with the respective antibodies against these chemokines in the presence of conditioned media. Neutralization with CCL5 antibody blocked the increase in the RANKL/OPG ratio in hFOB1.19 osteoblastic cells stimulated with A549 cell-derived CM. Treatment with CCL19 or CXCL11 antibody increased the RANKL/OPG ratio (Figure 1D and Supplementary Figure 4A). CCL5, CCL19, and CXCL11 antibodies had very similar effects on RANKL and OPG expression in osteoblastic cells stimulated with H838 cell-derived CM compared with osteoblastic cells exposed to A549 cell-derived CM (Figure 1E and Supplementary Figure 4B).

RUNX3 knockdown increased lung cancer-associated bone destruction in mice

To determine whether RUNX3 and RUNX3-regulated chemokines are associated with bone invasion in human

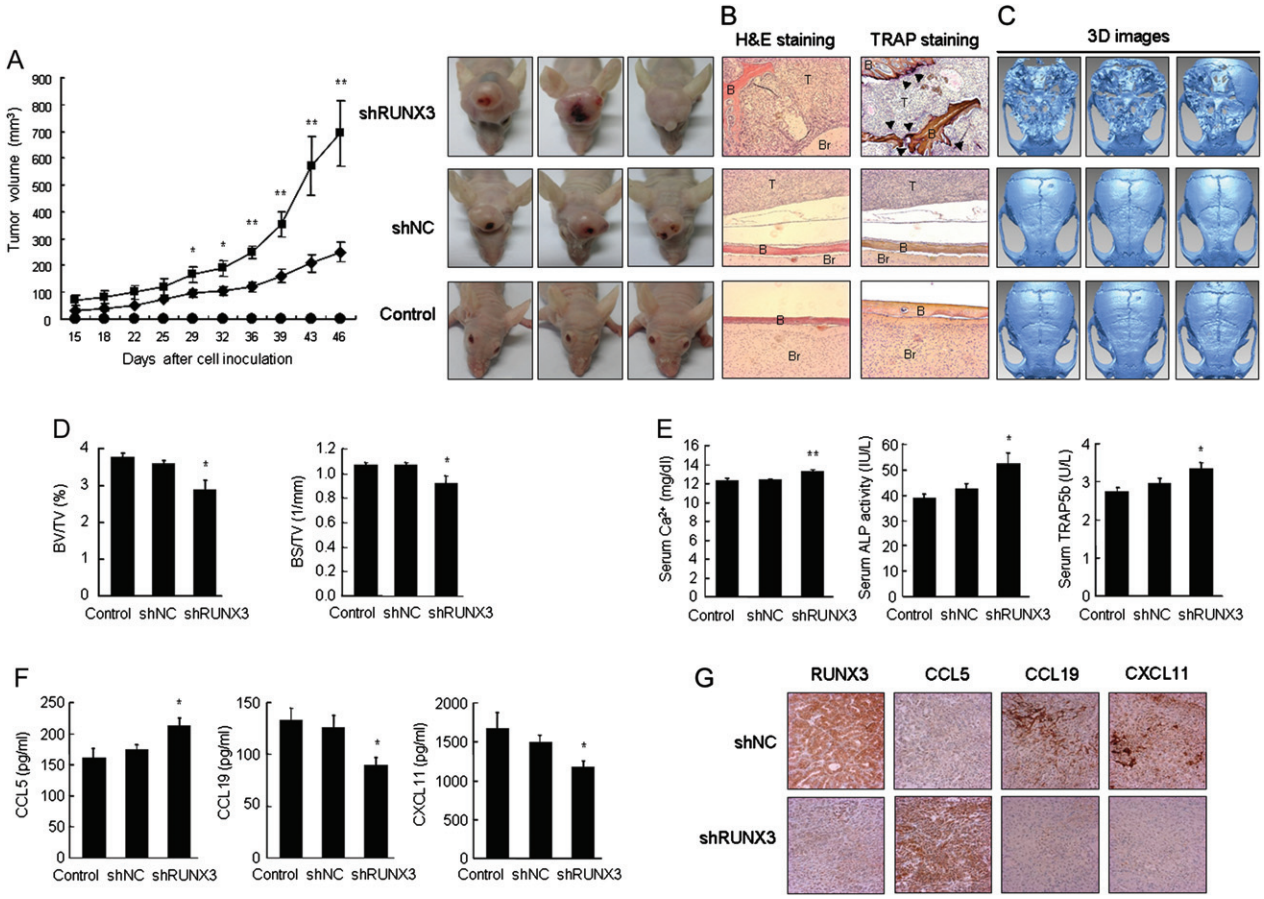

Figure 2. RUNX3 knockdown promoted tumour growth and caused bone destruction in mouse calvaria inoculated with NSCLC cells. shNC or shRUNX3 A549 cells (1×10^7 per 100 µl of PBS) were injected subcutaneously over the calvaria. Control mice were injected with PBS alone. On day 46, blood was collected and the mice were euthanized. (A) Tumour volumes and photos of tumour-bearing mouse heads. (B) H&E and TRAP staining of calvarial tissues. T = tumour; B = bone; Br = brain. Arrowheads denote osteoclasts (original magnification × 100). (C) 3D images were reconstructed from the 2D images of µCT using the software supplied with the instrument. (D) Bone morphometric parameters BV/TV (%) and BS/TV (1/mm) in mouse calvaria using µCT. (E) Serum levels of bone turnover markers Ca^{2+}, ALP, and TRAP5b, and (F) RUNX3-regulated chemokines. (G) Immunohistochemical analyses of RUNX3, CCL5, CCL19, and CXCL11 in the tumour tissues of mouse calvaria (original magnification × 200). Means ± SE. *$p < 0.05$, **$p < 0.005$ versus shNC A549 cell-inoculated mice.

lung cancer, we established two murine models. In mice in which A549 lung cancer cells were subcutaneously injected onto the surface of calvaria, tumour volumes increased more dramatically in response to RUNX3 knockdown (Figure 2A). Histological examination indicated that invasive tumour growth and severe bone resorption occurred in mice inoculated with shRUNX3 cells, whereas cancer cell invasion and osteolysis were hardly detected in mice inoculated with shNC cells. TRAP staining demonstrated that bone-resorbing osteoclasts (dark brown) were produced at the tumour–bone interface in the calvaria of shRUNX3 cell-inoculated mice compared with shNC cell-inoculated mice (Figure 2B). shRUNX3 cell-mediated osteolysis was confirmed via reconstructed 3D images of the μCT data (Figure 2C) as well as significant reductions in bone morphometric parameters, per cent bone volume (bone volume/tissue volume, BV/TV), and bone surface density (bone surface/tissue volume, BS/TV) in the calvaria inoculated with RUNX3-knockdown cells (Figure 2D). Additionally, the serum levels of calcium, ALP, and TRAP5b (markers of bone turnover) were significantly elevated in the shRUNX3 cell-inoculated mice (Figure 2E). Consistent with the results of the *in vitro* study, the serum level of CCL5 was significantly increased and those of CCL19 and CXCL11 were significantly decreased in the shRUNX3 cell-inoculated mice (Figure 2F). Using immunohistochemical analysis, we verified the increased expression of CCL5 and reduced expression of CCL19 and CXCL11 in tumour tissues from shRUNX3 cell-inoculated mice compared with shNC cell-inoculated mice (Figure 2G).

The intratibial injection of cancer cells in mice has been known to cause bone lesions similar to those observed in cancer patients [23]. Radiophotography and 3D images of the μCT data showed that osteolytic lesions were induced in the tibiae of shNC cell-injected mice and that RUNX3-knockdown cells aggravated osteolysis (Figure 3A). In bone morphometric analyses of the tibiae, the per cent bone volume (BV/TV), bone surface density (BS/TV), trabecular thickness (Tb.Th), and trabecular number (Tb.N) decreased, while the trabecular separation (Tb.Sp) and structure model index (SMI) increased in shNC cell-injected mice compared with control mice. RUNX3 knockdown resulted in a greater reduction of BV/TV, BS/TV, Tb.Th, and Tb.N, and a greater elevation of Tb.Sp and SMI (Figure 3B). Histological examination revealed that shRUNX3 cells invaded the tibiae more aggressively than shNC cells and that tumour volumes were significantly increased in shRUNX3 cell-inoculated mice compared with shNC cell-inoculated mice. Increased numbers of TRAP-positive mature osteoclasts were present within the bone surface close to the invasive tumour in the shRUNX3 cell-inoculated tibiae compared with the shNC cell-inoculated tibiae (Figure 3C). The serum levels of calcium, ALP, and TRAP5b were also significantly increased in shRUNX3 cell-inoculated mice compared with shNC cell-inoculated mice (Figure 3D). CCL5 was significantly elevated and CCL19 and CXCL11 did not change significantly in the sera of shRUNX3 cell-inoculated mice (Figure 3E). Immunohistochemical analysis showed that CCL5 increased substantially, whereas CCL19 and CXCL11 decreased in response to RUNX3 knockdown (Figure 3F). However, RANKL and OPG (Supplementary Figure 5A) as well as RUNX2 (Supplementary Figure 5B) did not show measurable changes after RUNX3 knockdown in both murine models. Therefore, the presence of osteolytic lesions caused by lung cancer cells was closely associated with RUNX3-regulated CCL5, CCL19, and CXCL11, as well as the expression of RUNX3.

CCL5 stimulated the proliferation, migration, and invasion of NSCLC cells

We evaluated the effects of CCL5, CCL19, and CXCL11 on lung cancer. Cell viability, BrdU incorporation, cell migration, and cell invasion were increased in both shNC and shRUNX3 cells treated with CCL5, and this increase was greater in shRUNX3 cells than in shNC cells (Figure 4). By contrast, CCL19 and CXCL11 did not substantially affect the proliferation, migration, or invasion of either shNC or shRUNX3 cells.

CCL5, CCL19, and CXCL11 regulated osteoblastic RANKL and OPG expression and RANKL-induced differentiation of osteoclast precursors

Next, we determined the effect of CCL5, CCL19, and CXCL11 on the osteoclastogenesis-associated factors RANKL and OPG in hFOB1.19 osteoblastic cells. Real-time RT-PCR (Figure 5A and Supplementary Figure 6A) and western blot analysis (Figure 5B and Supplementary Figure 6B) revealed that CCL5 caused an increase in the RANKL/OPG ratio via the up-regulation of *RANKL* mRNA and protein expression and/or the down-regulation of *OPG* mRNA and protein expression in a dose-dependent manner. In contrast, CCL19 and CXCL11 decreased the RANKL/OPG ratio by down-regulating *RANKL* mRNA and protein expression and/or up-regulating *OPG* mRNA and protein expression. However, CCL5, CCL19, and CXCL11 did not affect RANKL and OPG in A549 (Supplementary Figure 7A) and H838 NSCLC cells (Supplementary Figure 7B).

We further examined whether CCL5, CCL19, and CXCL11 could directly induce osteoclast formation in BMMs. In BMMs treated with CCL5, CCL19, or CXCL11 for 5 days, CCL5 increased cell viability by 15% at a concentration of 7 μM ($p < 0.05$); however, CCL19 and CXCL11 did not affect cell viability. CCL5 also stimulated the formation of TRAP-positive osteoclasts by 15% at a concentration of 7 μM; however, at the same concentration, CCL19 and CXCL11 markedly decreased osteoclast formation by 32% and 41%, respectively, in RANKL-treated BMMs. Interestingly, CCL5, CCL19, or CXCL11 alone did not induce osteoclast differentiation from BMMs in the absence of RANKL (Figure 5C).

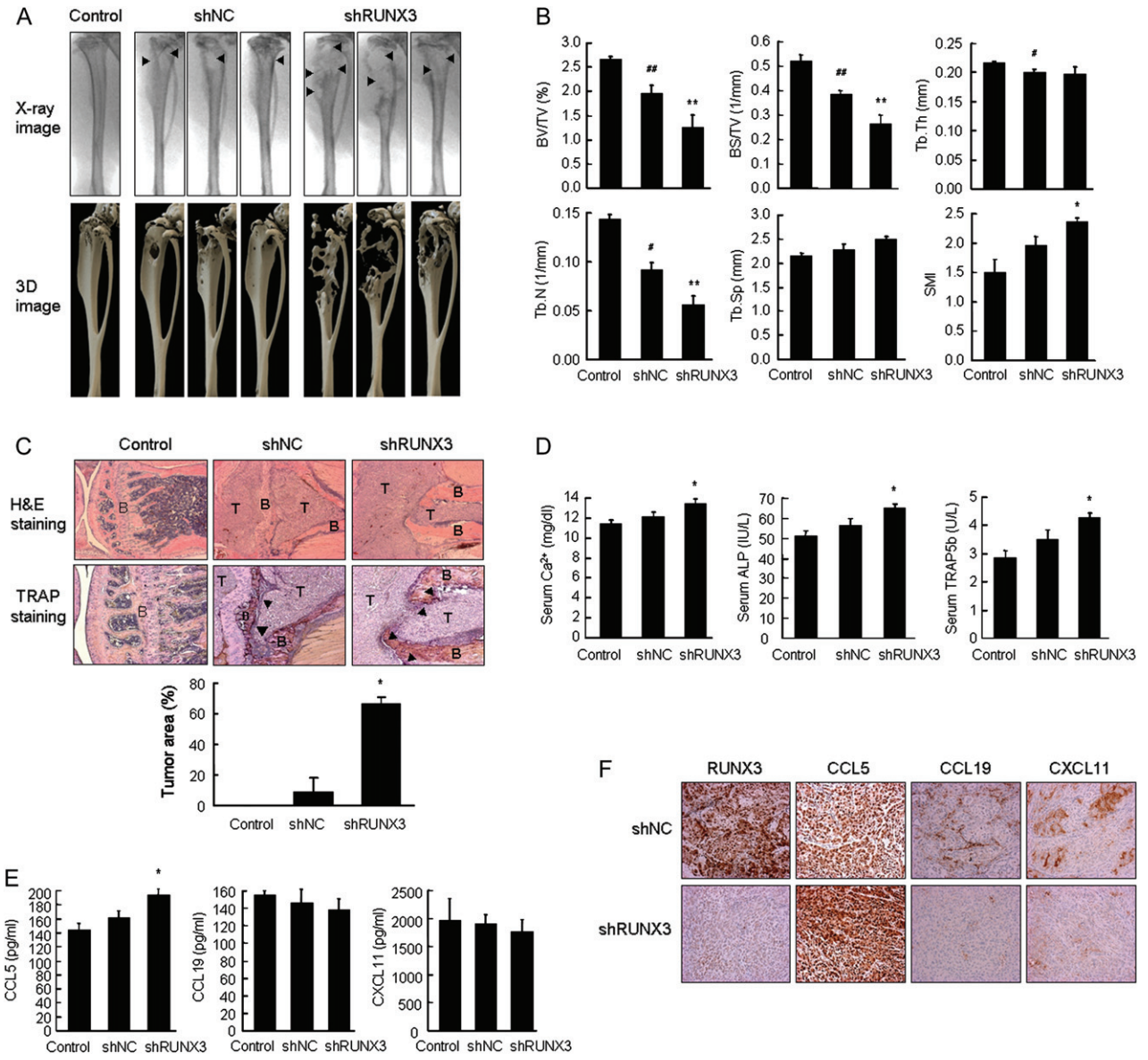

Figure 3. RUNX3 knockdown aggravated bone destruction in mouse tibiae inoculated with NSCLC cells. A549 cells (1×10^6 cells per 50 µl of HBSS) were injected into the bone marrow of the tibiae through the femorotibial cartilage. Control mice were injected with HBSS alone. On day 49, the mouse tibiae were analysed using µCT and blood and tibiae were collected. (A) Radiophotographs and 3D images of µCT data from the tibiae. Arrowheads indicate osteolytic foci. (B) The bone morphometric parameters of mouse tibia were determined using µCT. (C) H&E (original magnification × 50) and TRAP staining (original magnification × 100). Tumour area was measured in H&E-stained tissues. T = tumour; B = bone. Arrowheads denote osteoclasts (D, E) Serum levels of bone turnover markers Ca^{2+}, ALP, and TRAP5b, and RUNX3-regulated chemokines. (F) RUNX3, CCL5, CCL19, and CXCL11 in tumour tissues of mouse tibiae were detected via immunohistochemical analysis (original magnification × 200). Means ± SE. $^{\#}p < 0.05$, $^{\#\#}p < 0.005$ versus control mice; $^{*}p < 0.05$ versus shNC A549 cell-inoculated mice.

Discussion

The majority of advanced-stage lung cancer patients die within 18 months of diagnosis; the median survival time of lung cancer patients with bone metastases is less than 1 year [1,24]. Bone metastases are usually diagnosed using bone imaging techniques; however, the current imaging methods are not sufficiently sensitive for the detection of bone metastases and can also be invasive and expensive [25]. A number of clinical trials have focused on factors derived from bone metabolism rather than tumour-derived factors, and bisphosphonates, bone resorption inhibitors, and denosumab, a monoclonal antibody against RANKL, have been applied for the treatment of patients with bone metastases [25,26]. However, bisphosphonates and RANKL-targeted therapies can cause serious adverse events such as hypocalcaemia, osteonecrosis of the jaw, and renal toxicity. Thus, there is a significant need for the prediction of bone metastasis and the establishment of more effective therapeutic strategies. More recent studies have focused on cancer-derived factors that stimulate differentiation and activation of osteoclasts either directly or through osteoblasts [10,27]. We

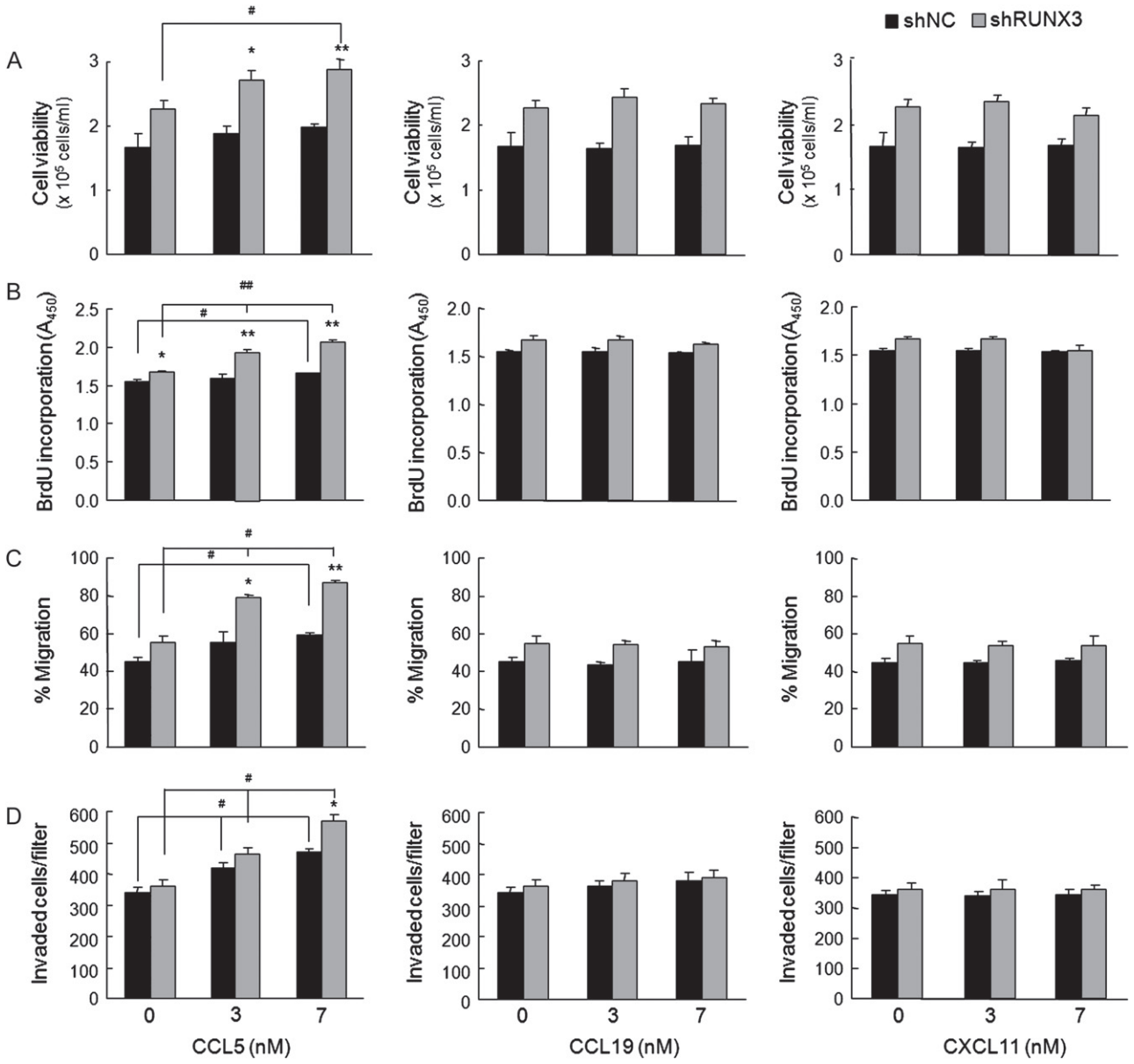

Figure 4. CCL5 enhanced the proliferation, migration, and invasion of NSCLC cells. (A) Trypan blue exclusion of A549 (1×10^5 cells per ml) treated with the indicated concentrations of human CCL5, CCL19, or CXCL11 for 48 h. (B) BrdU incorporation of cells (1×10^4 cells per well) exposed to the indicated concentrations of chemokines for 24 h. (C) Cell migration in RPMI1640 medium containing 2% FBS, 10 μg/ml mitomycin C, and the indicated concentrations of chemokines for 24 h. (D) A549 (1×10^5 cells per 0.1 ml) invasion through Matrigel-coated filter. Cells were suspended in serum-free medium containing 0.01% BSA. The lower chamber was filled with 600 μl of medium containing 10% FBS and/or human chemokines at the indicated concentrations. Invaded cells were counted after 48 h. Means ± SE. $^{\#}p < 0.05$, $^{\#\#}p < 0.005$ versus cells without chemokines; $^{*}p < 0.05$, $^{**}p < 0.005$ versus shNC cells.

assessed whether the cancer-derived factors RUNX3 and RUNX3-regulated chemokines could be useful for the detection and management of lung cancer bone metastasis.

We found that RUNX3 knockdown in RUNX3-expressing NSCLC cells increased the RANKL/OPG ratio in osteoblastic cells, rather than affecting the proliferation, migration, and invasion of the cancer cells themselves, indicating that these lung cancer cells secreted factors that modified RANKL and OPG expression in osteoblastic cells and that the expression of these factors was regulated by RUNX3. The relative ratio of RANKL/OPG in the bone marrow microenvironment is one of the principal factors that regulate osteoclast formation and activation [28]. In patients with cancers that metastasize to bone, an increased RANKL/OPG ratio results in a higher risk of osteolytic lesions and mortality [29–31].

Chemokines act as key mediators that facilitate the interplay between tumour cells and their surrounding cells in the microenvironment [32], and some chemokines play critical roles in bone destruction via cancer cells with bone tropism [33]. Therefore, we analysed the expression of chemokines and their receptors in response to RUNX3 knockdown to determine the factors that regulate osteoblastic RANKL

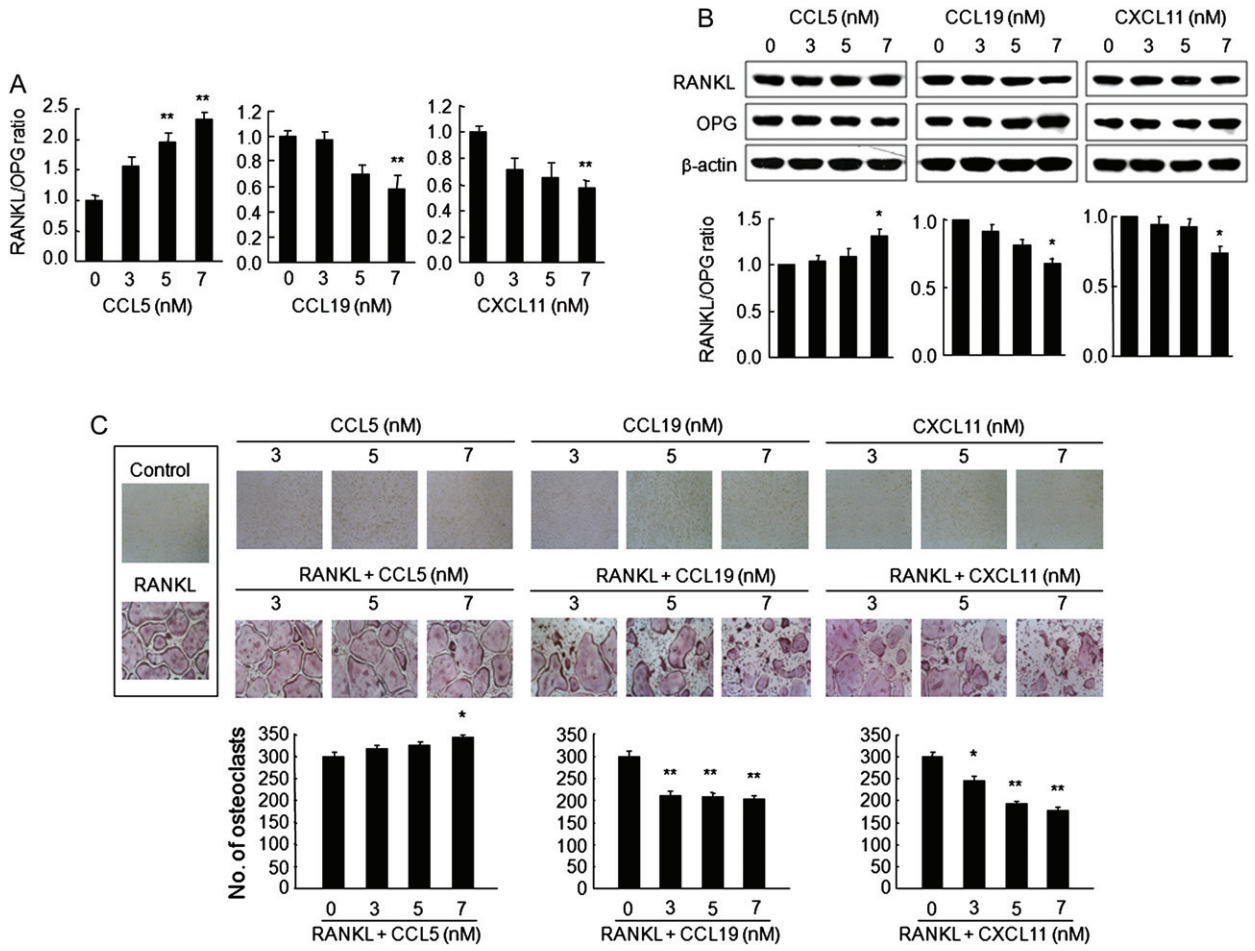

Figure 5. CCL5, CCL19, and CXCL11 altered RANKL and OPG expression in osteoblastic cells and RANKL-induced osteoclast differentiation in BMMs. Human osteoblastic hFOB1.19 cells were treated with the indicated concentrations of human CCL5, CCL19, or CXCL11 for 6 h. (A) *RANKL* and *OPG* mRNA analysed via qRT-PCR. GAPDH was used as an endogenous control. (B) Western blots of total cell lysates (representative of three independent experiments). β-actin served as a loading control. Graphs show densitometric intensity ratios of RANKL/OPG after normalization. Means ± SE; $^{*}p < 0.01$ versus osteoblastic cells without chemokines. (C) Mouse BMMs (5×10^4 cells per well) cultured for 5 days in α-MEM containing 10% FBS and 30 ng/ml M-CSF, in the absence or presence of CCL5, CCL19, or CXCL11 at the indicated concentrations and in the absence (control) or presence of 100 ng/ml RANKL. TRAP staining was performed to detect osteoclasts (original magnification × 100). TRAP-positive multinucleated cells (≥3 nuclei) were counted as osteoclasts. Means ± SE; $^{*}p < 0.05$, $^{**}p < 0.005$ versus RANKL-treated BMMs.

and OPG expression in lung cancer cell-derived conditioned media. RUNX3 knockdown resulted in the up-regulation of *CCL5* and *TCP10* mRNA and the down-regulation of *CXCL11*, *CCL19*, and *HCAR1* mRNA in A549 cells. CCL5 contributes to the migration and invasion of human lung, breast, and oral cancer cells [34–37]. Clinical evidence has demonstrated that elevated levels of tissue or plasma CCL5 are useful for predicting survival as well as unfavourable outcomes in cancer patients [38–40]. Among the down-regulated chemokines in RUNX3-knockdown A549 cells, CCL19 showed IFN-γ-dependent anti-tumour responses in a murine lung cancer model and reduced tumourigenicity in a murine ovarian carcinoma model [41,42]. CXCL11 is characterized by its anti-tumoural and anti-inflammatory activities because it acts as an angiostatic regulator and mediates the infiltration of T lymphocytes and natural killer cells [43,44]. The roles of hydroxycarboxylic acid receptor 1 (HCAR1) and T-complex 10 homologue (TCP10) in human cancer progression remain unknown. Thus, we selected CCL5, CCL19, and CXCL11 as NSCLC-derived factors that influence the osteoblastic RANKL/OPG ratio.

We confirmed that the amount of secreted CCL5 increased, while that of CCL19 and CXCL11 decreased in response to RUNX3 knockdown in both NSCLC cell lines. Neutralization with specific antibodies indicated that these chemokines may serve as NSCLC-derived factors regulating the RANKL/OPG ratio in osteoblastic cells: treatment with CCL5 antibody reduced the conditioned medium-induced increase in the RANKL/OPG ratio, whereas treatment with antibodies against CCL19 and CXCL11 increased the RANKL/OPG ratio. Additionally, RUNX3 knockdown increased tumour volumes and induced severe osteolytic lesions in the calvaria and tibiae of A549 cell-injected mice, as supported by examinations of bone morphometric parameters, the serum levels of biochemical bone turnover markers, and histological analyses of bone invasion. Serum and tissue levels of CCL5 were

elevated, while those of CCL19 and CXCL11 were reduced in response to RUNX3 knockdown. These results suggest that the loss of RUNX3 may exacerbate bone invasion and osteolysis, and that this phenomenon is closely associated with the induction of CCL5 and the inhibition of CCL19 and CXCL11 in NSCLC cells.

Based on these results, we further investigated the effects of CCL5, CCL19, and CXCL11 on NSCLC cells, osteoblasts, and osteoclasts, which participate in the vicious cycle of lung cancer-induced bone destruction. CCL5 stimulated the proliferation, migration, and invasion of RUNX3-knockdown lung cancer cells compared with RUNX3-expressing cells, whereas CCL19 and CXCL11 had no effect. CCL5 substantially increased the RANKL/OPG ratio, while CCL19 and CXCL11 decreased this ratio in osteoblastic cells. Moreover, CCL5 stimulated osteoclast formation via the increased viability of BMMs, whereas CCL19 and CXCL11 reduced osteoclast differentiation in RANKL-treated BMMs. These results indicate that lung cancer cell-derived CCL5 may act as an osteolytic factor but CCL19 and CXCL11 may possess anti-osteoclastogenic activity.

Finally, we attempted to estimate the clinical significance of RUNX3 and chemokines. Because lung metastases to bone are rarely resected and were not available for study, we analysed TCGA microarray data and online bioinformatics tools in KM plotter [45]. *RUNX3* expression was significantly lower in NSCLC tissues than in normal tissues, and in advanced stages (stages III and IV) with distant metastasis than in early stages (stages I and II) (Supplementary Figure 8A). The 5-year overall survival was significantly higher in patients with high levels of *RUNX3* and RUNX3-regulated chemokines (Supplementary Figure 8B). High levels of *CCL5* and low levels of *RUNX3*, *CCL19*, and *CXCL11* may be correlated with poor post-progression survival (Supplementary Figure 8C).

CCL5 promotes the migration, invasion, and metastasis in lung, breast, and prostate cancer cells [34–36,46]. In breast and gastric cancer, higher CCL5 expression increased significantly the risk for disease progression and reduced the overall survival of patients [38,47]. Plasma CCL5 levels were higher in the order of stages IV, III, II, and I in patients with breast or cervical cancer [48]. In contrast, stage I lung adenocarcinoma patients with lower *CCL5* mRNA expression had a higher mortality [49]. This difference in tumour behaviour may be worthy of future study. Further studies are also required to obtain more significant data in clinical samples.

In conclusion, RUNX3 and the RUNX3-regulated chemokines CCL5, CCL19, and CXCL11 are closely associated with NSCLC-induced osteolysis. Therefore, RUNX3 expression and the levels of related chemokines can serve as predictive markers and future therapeutic targets for lung cancer-induced bone destruction.

Acknowledgments

We thank Chae-Eun Lee from the Oral Science Research Institute for technical assistance with μCT. This research was supported by the Basic Science Research Program through the National Research Foundation of Korea (NRF) funded by the Ministry of Education (2013R1A1A2009011).

Author contributions

HJK performed all experiments, interpreted data, and wrote the first draft of the manuscript. JHP, SKL, and KRK participated in *in vivo* studies and data interpretation. KKP and WYC conceived the concept, designed experiments, interpreted data, and wrote the manuscript.

References

1. Coleman RE. Metastatic bone disease: clinical features, pathophysiology and treatment strategies. *Cancer Treat Rev* 2001; **27:** 165–176.
2. Al Husaini H, Wheatley-Price P, Clemons M, *et al.* Prevention and management of bone metastases in lung cancer: a review. *J Thorac Oncol* 2009; **4:** 251–259.
3. Mundy GR. Metastasis to bone: causes, consequences and therapeutic opportunities. *Nature Rev Cancer* 2002; **2:** 584–593.
4. Teitelbaum SL, Ross FP. Genetic regulation of osteoclast development and function. *Nature Rev Genet* 2003; **4:** 638–649.
5. Roodman GD, Dougall WC. RANK ligand as a therapeutic target for bone metastases and multiple myeloma. *Cancer Treat Rev* 2008; **34:** 92–101.
6. Yin JJ, Selander K, Chirgwin JM, *et al.* TGF-beta signaling blockade inhibits PTHrP secretion by breast cancer cells and bone metastases development. *J Clin Invest* 1999; **103:** 197–206.
7. Lund AH, van Lohuizen M. RUNX: a trilogy of cancer genes. *Cancer Cell* 2002; **1:** 213–215.
8. Pratap J, Lian JB, Javed A, *et al.* Regulatory roles of RUNX2 in metastatic tumor and cancer cell interactions with bone. *Cancer Metastasis Rev* 2006; **25:** 589–600.
9. Subramaniam MM, Chan JY, Yeoh KG, *et al.* Molecular pathology of RUNX3 in human carcinogenesis. *Biochim Biophys Acta* **2009**; 1796: 315–331.
10. Chung JH, Lee HJ, Kim BH, *et al.* DNA methylation profile during multistage progression of pulmonary adenocarcinomas. *Virchows Arch* 2011; **459:** 201–211.
11. Lee YS, Lee JW, Jang JW, *et al.* Runx3 inactivation is a crucial early event in the development of lung adenocarcinoma. *Cancer Cell* 2013; **24:** 603–616.
12. Yu GP, Ji Y, Chen GQ, *et al.* Application of RUNX3 gene promoter methylation in the diagnosis of non-small cell lung cancer. *Oncol Lett* 2012; **3:** 159–162.
13. Yoshida CA, Yamamoto H, Fujita T, *et al.* Runx2 and Runx3 are essential for chondrocyte maturation, and Runx2 regulates limb growth through induction of Indian hedgehog. *Genes Dev* 2004; **18:** 952–963.
14. Jin Z, Han YX, Han XR. Loss of RUNX3 expression may contribute to poor prognosis in patients with chondrosarcoma. *J Mol Histol* 2013; **44:** 645–652.
15. Raman D, Sobolik-Delmaire T, Richmond A. Chemokines in health and disease. *Exp Cell Res* 2011; **317:** 575–589.
16. Balkwill F. Cancer and the chemokine network. *Nature Rev Cancer* 2004; **4:** 540–550.

17. Kang Y, Esposito M. Targeting tumor–stromal interactions in bone metastasis. *Pharmacol Ther* 2014; **141:** 222–223.
18. Hsu YL, Hung JY, Ko YC, *et al.* Phospholipase D signaling pathway is involved in lung cancer-derived IL-8 increased osteoclastogenesis. *Carcinogenesis* 2010; **31:** 587–596.
19. Nakamura ES, Koizumi K, Kobayashi M, *et al.* RANKL-induced CCL22/macrophage-derived chemokine produced from osteoclasts potentially promotes the bone metastasis of lung cancer expressing its receptor CCR4. *Clin Exp Metastasis* 2006; **23:** 9–18.
20. Park SY, Kim HJ, Kim KR, *et al.* Betulinic acid, a bioactive pentacyclic triterpenoid, inhibits skeletal-related events induced by breast cancer bone metastases and treatment. *Toxicol Appl Pharmacol* 2014; **275:** 152–162.
21. Kim KR, Kim HJ, Lee SK, *et al.* 15-deoxy-$\Delta^{12,14}$-prostaglandin J_2 inhibits osteolytic breast cancer bone metastasis and estrogen deficiency-induced bone loss. *PLoS one* 2015; **10**: e0122764.
22. Jun AY, Kim HJ, Park KK, *et al.* Tetrahydrofurofuran-type lignans inhibit breast cancer-mediated bone destruction by blocking the vicious cycle between cancer cells, osteoblasts and osteoclasts. *Invest New Drugs* 2014; **32:** 1–13.
23. Campbell JP, Merkel AR, Masood-Campbell SK, Models of bone metastasis. *J Vis Exp* 2012; e4260.
24. Gupta GP, Massague J. Cancer metastasis: building a framework. *Cell* 2006; **127:** 679–695.
25. Huang Q, Ouyang X. Biochemical-markers for the diagnosis of bone metastasis: a clinical review. *Cancer Epidemiol* 2012; **36:** 94–98.
26. Hirsh V. Targeted treatments of bone metastases in patients with lung cancer. *Front Oncol* 2014; **4:** 146.
27. Hung JY, Horn D, Woodruff K, *et al.* Colony-stimulating factor 1 potentiates lung cancer bone metastasis. *Lab Invest* 2014; **94:** 371–381.
28. Goranova-Marinova V, Goranov S, Pavlov P, *et al.* Serum levels of OPG, RANKL and RANKL/OPG ratio in newly-diagnosed patients with multiple myeloma. *Clinical correlations. Haematologica* 2007; **92:** 1000-1001.
29. Chen G, Sircar K, Aprikian A, *et al.* Expression of RANK/OPG in primary and metastatic human prostate cancer as markers of disease stage and functional regulation. *Cancer* 2006; **107:** 289–298.
30. Karapanagiotou EM, Terpos E, Dilana KD, *et al.* Serum bone turnover markers may be involved in the metastatic potential of lung cancer patients. *Med Oncol* 2010; **27:** 332–338.
31. Mountzios G, Terpos E, Syrigos K, *et al.* Markers of bone remodeling and skeletal morbidity in patients with solid tumors metastatic to the skeleton receiving the biphosphonate zoledronic acid. *Transl Res* 2010; **155:** 247–255.
32. O'Hayre M, Salanga CL, Handel TM, *et al.* Chemokines and cancer: migration, intracellular signaling and intercellular communication in the microenvironment. *Biochem J* 2008; **409:** 635–649.
33. Nannuru KC, Singh RK. Tumor–stromal interactions in bone metastasis. *Curr Osteoporos Rep* 2010; **8:** 105–113.
34. Karnoub AE, Dash AB, Vo AP, *et al.* Mesenchymal stem cells within tumour stroma promote breast cancer metastasis. *Nature* 2007; **449:** 557–563.
35. Borczuk AC, Papanikolaou N, Toonkel RL, *et al.* Lung adenocarcinoma invasion in *TGFβRII*-deficient cells is mediated by CCL5/RANTES. *Oncogene* 2008; **27:** 557–564.
36. Huang CY, Fong YC, Lee CY, *et al.* CCL5 increases lung cancer migration via PI3K, Akt and NF-kappaB pathways. *Biochem Pharmacol* 2009; **77:** 794–803.
37. Chuang JY, Yang WH, Chen HT, *et al.* CCL5/CCR5 axis promotes the motility of human oral cancer cells. *J Cell Physiol* 2009; **220:** 418–426.
38. Sima AR, Sima HR, Rafatpanah H, *et al.* Serum chemokine ligand 5 (CCL5/RANTES) level might be utilized as a predictive marker of tumor behavior and disease prognosis in patients with gastric adenocarcinoma. *J Gastrointest Cancer* 2014; **45:** 476–480.
39. Tsukishiro S, Suzumori N, Nishikawa H, *et al.* Elevated serum RANTES levels in patients with ovarian cancer correlate with the extent of the disorder. *Gynecol Oncol* 2006; **102:** 542–545.
40. Yaal-Hahoshen N, Shina S, Leider-Trejo L, *et al.* The chemokine CCL5 as a potential prognostic factor predicting disease progression in stage II breast cancer patients. *Clin Cancer Res* 2006; **12:** 4474–4480.
41. Hillinger S, Yang SC, Zhu L, *et al.* EBV-induced molecule 1 ligand chemokine (ELC/CCL19) promotes IFN-gamma-dependent antitumor responses in a lung cancer model. *J Immunol* 2003; **171:** 6457–6465.
42. Mandai M, Hamanishi J, Abiko K, *et al.* Suppression of metastatic murine ovarian cancer cells by transduced embryonic progenitor cells. *Horm Cancer* 2010; **1:** 291–296.
43. Hensbergen PJ, Wijnands PG, Schreurs MW, *et al.* The CXCR3 targeting chemokine CXCL11 has potent antitumor activity *in vivo* involving attraction of CD8+ T lymphocytes but not inhibition of angiogenesis. *J Immunother* 2005; **28:** 343–351.
44. Yang X, Chu Y, Wang Y, *et al.* Vaccination with IFN-inducible T cell alpha chemoattractant (ITAC) gene-modified tumor cell attenuates disseminated metastases of circulating tumor cells. *Vaccine* 2006; **24:** 2966–2974.
45. Győrffy B, Surowiak P, Budczies J, *et al.* Online survival analysis software to assess the prognostic value of biomarkers using transcriptomic data in non-small-cell lung cancer. *PLoS One* 2013; **8:** e82241.
46. Kato T, Fujita Y, Nakane K, *et al.* CCR1/CCL5 interaction promotes invasion of taxane-resistant PC3 prostate cancer cells by increasing secretion of MMPs 2/9 and by activating ERK and Rac signaling. *Cytokine* 2013; **64:** 251–257.
47. Zhang Y, Yao F, Yao X, *et al.* Role of CCL5 in invasion, proliferation and proportion of CD44+/CD24− phenotype of MCF-7 cells and correlation of CCL5 and CCR5 expression with breast cancer progression. *Oncol Rep* 2009; **21:** 1113–1121.
48. Niwa Y, Akamatsu H, Niwa H, *et al.* Correlation of tissue and plasma RANTES levels with disease course in patients with breast or cervical cancer. *Clin Cancer Res* 2001; **7:** 285–289.
49. Moran CJ, Arenberg DA, Huang CC, *et al.* RANTES expression is a predictor of survival in stage I lung adenocarcinoma. *Clin Cancer Res* 2002; **8:** 3803–3812.

SUPPORTING INFORMATION ON THE INTERNET

The following supporting information may be found in the online version of this article:

Supplementary materials and methods.

Table S1. Altered gene expression of chemokines and their receptors via RUNX3 knockdown in A549 lung cancer cells.

Table S2. List of primer sequences.

Figure S1. Effect of RUNX3 knockdown on the proliferation, migration, and invasion in NSCLC cells.

Figure S2. Effect of RUNX3 knockdown on mRNA and protein expressions of CCL5, CCL19, and CXCL11 in NSCLC cells.

Figure S3. Effect of RUNX3 knockdown on mRNA and protein expressions of CCL5, CCL19, and CXCL11 receptors in NSCLC cells.

Figure S4. RANKL and OPG expression in osteoblastic cells exposed to NSCLC-derived CM and neutralizing antibody against CCL5, CCL19 or CXCL11.

Figure S5. RANKL, OPG and RUNX2 expression in tissues of mice inoculated with shNC or shRUNX3 cells.

Figure S6. RANKL and OPG expression in osteoblastic cells treated with CCL5, CCL19 or CXCL11.

Figure S7. Effect of CCL5, CCL19, and CXCL11 on the expression of RANKL and OPG in NSCLC cells.

Figure S8. The relationship between the expression level of RUNX3 or chemokines and lung cancer.